

# Particulate-fibre-reinforced glass matrix hybrid composites

K. P. GADKAREE

Corning Incorporated, Sullivan Park, Corning, New York 14831, USA

This study extends the concept of hybridization of glass matrix composites to fibre and particulate reinforcements. Hybridization of Nicalon<sup>®</sup>-glass matrix composites with silicon carbide particulates of mean diameters of 0.77, 1.5 and 6  $\mu\text{m}$  was studied. The microcrack stress, transverse strength and interlaminar strengths improved significantly on hybridization. At the optimum loading of 7.5 wt % for 6  $\mu\text{m}$  particle size the microcrack stress increased by 62%, transverse strength by 650% and interlaminar shear strength by 200%. The ultimate strength declined for this composite by 6%. The decline in ultimate properties was attributed to the damaged graphitic skin at the particle-fibre contact points.

## 1. Introduction

Nicalon<sup>®</sup> silicon oxycarbide fibre-reinforced glass and glass-ceramics are being extensively studied for high-temperature aerospace applications [1-5]. The glass or glass-ceramic matrix has a lower failure strain ( $\sim 0.1\%$ ) compared to the fibre ( $\sim 1\%$ ). This difference in failure strains results in microcracking of the matrix at strains much lower than the ultimate failure strain of the composite, which is governed by the fibre. The composite consists of a severely cracked matrix held together by fibres beyond the microcrack point. The microcracking phenomenon leads to severe oxidation embrittlement problems at high temperatures. In addition to the embrittlement problem, there is a significant loss in stiffness associated with microcracking. Under cyclic loading conditions the microcracking of the brittle matrix may also result in severe fatigue degradation. These considerations will probably limit the use of the composites to a design stress level at a certain low percentage of the microcrack stress. Because the microcrack stress is significantly lower ( $\sim 30\%$ ) than the ultimate strength of the composite, the high strength of the fibre is not fully utilized. The glass and glass-ceramic composites also have the problems associated with the fundamental anisotropic nature of the composites, such as low transverse and interlaminar shear strengths. These properties can be design-limiting in many applications. It is thus desirable to increase the microcrack stress and strains and the off-axis properties.

In an earlier paper [6] the concept of hybridization of the glass or glass-ceramic matrix composites was proposed. It was postulated that addition of silicon carbide whiskers to the glass matrix would result in substantial increases in microcrack point as well as off-axis properties. Data showed that the hybridization resulted in very significant improvements in microcrack yield stress and strain, interlaminar shear strength and transverse strength over that of the non-hybrid systems. These improvements were attributed

to the increase in the fracture energy and the strength of the matrix. It was also found that at high whisker loadings there was significant fibre damage resulting in decreases in ultimate strength and strain compared to a non-hybrid system. The fibre damage occurs because of the contact between the fibres and the sharp corners of hard whiskers during prepregging and hot pressing. It might be possible to reduce the fibre damage if sharp whisker corners could be eliminated. Replacement of whiskers by spherical particles might accomplish this reduction in fibre damage. Spherical fillers might also result in better consolidation of composites compared to whisker-containing hybrids.

The effect of spherical glass particles on fracture energies of brittle thermosets such as epoxies and unsaturated polyesters has been the subject of a number of studies [7-9]. Fracture propagation energies were found to increase significantly as a result of incorporation of the fillers. The fracture energy was maximum at an optimum filler loading, while the fracture energy of the composite also increased with increasing particle size.

It has been shown [6] that the microcrack point is a direct function of the matrix fracture energy and is strongly affected by changes in it. Because addition of fillers also increases the fracture energy of the matrix, improvements in microcrack point can be expected by addition of fillers to the matrix. Fillers such as silicon carbide and alumina which can withstand the composite processing temperatures may be used. This paper reports the work done with an alkaline earth alumino silicate glass matrix (Corning Code 1723), Nicalon<sup>®</sup> silicon oxycarbide fibres and silicon carbide particulates.

## 2. Theory

Friedel [7] first advanced the concept that a crack front possesses line energy. In essence, this concept

associates the increased strain energy of a cracked body with the periphery of a crack, rather than the crack as a whole. Based on this concept, Lange [8] developed a model suggesting that the increased crack front length could significantly contribute to the fracture energy of a composite containing brittle particulate fillers. The crack front, when propagating through the material, becomes temporarily pinned and is slowed down at an inhomogeneity. The pinned crack front bows forward between pinning points, until it forms semicircular segments of diameter equal to the spacing between the particles. The segments then overlap behind the pinning points, and the crack front breaks away. The crack front increases its length as it bows between each pair of pinning positions.

Lange and Redford [9], based on microscopic examination of fracture surfaces, proposed that, when loading of filler particles in a composite exceeds the optimum loading, the particles are too closely spaced for effective crack front enlargement to occur. Brautman and Sahu [10] proposed that the force to move the crack front was proportional to the inverse of its radius of curvature. At filler loadings above the optimum, it becomes easier to break interfacial bonds than to bend the crack front to a breakaway position. The optimum interparticle distance, which is determined by the particle size as well as volume fraction of particles, would then be unique for a given system, because of the differences in matrix fracture energies and differences in strength of the bond between the filler and the matrix. An *a priori* prediction of improvements in fracture energy from addition of fillers is thus difficult.

If the dispersed particles are of higher elastic modulus than that of the matrix and strong particle-matrix bonding exists, stress transfer from matrix to the particles will take place and the strength of the system will increase. This, in turn, should result in increases in transverse and interlaminar strengths of the hybrids as discussed earlier [6].

It was found that the well known ACK theory for well-bonded brittle fibre-brittle matrix composites predicts microcrack stresses which closely approximate the experimental data for whisker-fibre hybrids [6]. It is expected that the same model will be applicable in this case. Equation 4 in Reference 6 may be rewritten as

$$\frac{\sigma_{mcy_1}}{\sigma_{mcy_2}} = \frac{K_{IC_1}}{K_{IC_2}} \left( \frac{G_{m_1}}{G_{m_2}} \frac{E_{m_2}}{E_{m_1}} \frac{E_{c_2}}{E_{c_1}} \right)^{1/4} \quad (1)$$

where  $K_{IC}$  is the fracture toughness,  $\sigma_{mcy}$  the microcrack stress,  $E_m$  the matrix modulus, and  $E_c$  the composite modulus. The microcrack stresses thus should be directly proportional to the fracture toughness of the matrix.

An estimate of transverse strength improvement may be obtained by

$$\sigma_c = \frac{\sigma_M}{S} \quad (2)$$

where  $\sigma_M$  is the matrix strength and  $S$  is the stress concentration factor.

$$S = \frac{1 - V_f(1 - E_f/E_m)}{1 - (4V_f/\bar{\Lambda})^2 (1 - E_f/E_m)} \quad (3)$$

where  $V_f$  is the volume fraction of fibre.

Interlaminar shear strength is also expected to increase because of the expected increase in matrix strength. Thus it is concluded that the microcrack stresses of filler-fibre hybrid composites would be higher than for fibre composites alone if the filler is strongly bonded to the matrix, resulting in pinning of the crack front. The degree of improvement will depend on the volume fraction of the filler, the particle size and the particle size distribution of the filler.

If the filler has a higher modulus than the matrix, substantial improvements in the transverse strength will result due to increase in matrix strength; interlaminar shear strength would also be expected to increase.

Based on the foregoing considerations, it was decided to carry out experiments with silicon carbide particles of various sizes and at various volume fractions at each particle size to define the optimum system in terms of the composite mechanical properties. Corning Code 1723 glass was chosen because of the ease of processing.

### 3. Experimental Materials and Processing

The glass matrix used for the experiment was Corning Incorporated's Code 1723 alkaline earth alumino silicate glass. The fibres were Nilcalon<sup>®</sup> silicon oxycarbide NLM202 fibres from Nippon Carbon. The particulate silicon carbide filler was obtained from ICD Group Inc., New York, N.Y. USA.

The particulate silicon carbide was mixed with glass powder by ball milling in isopropanol in appropriate proportions. The mixture was filtered and dried. The Nilcalon<sup>®</sup> fibres were then impregnated with this mixture using a polymeric binder system. The uniaxial prepreg plies were stacked, the binder burned off, and then hot pressed in graphite dies at an appropriate temperature to attain full consolidation.

Hybrid composites were fabricated with three different mean particle size silicon carbide particulates, respectively. These particulates were claimed to be spherical silicon carbide particulates with 0.7, 1.5 and 6  $\mu\text{m}$  mean diameters. Some experiments using 5  $\mu\text{m}$  mean particle size abrasive grain silicon carbide were also completed to compare results. Figs 1-3 show scanning electron micrographs of these particles. The particles do not have a spherical shape as claimed by the supplier. Comparing these particles with SiC abrasive powder particles shown in Fig. 4, it is seen that the "spherical" particles have relatively fewer sharp edges and corners. These features might be expected to result in less damage infliction to the fibres during processing. Although the particles are not spherical in nature, they are referred to as spherical particles to avoid confusion with the abrasive grain silicon carbide particles.

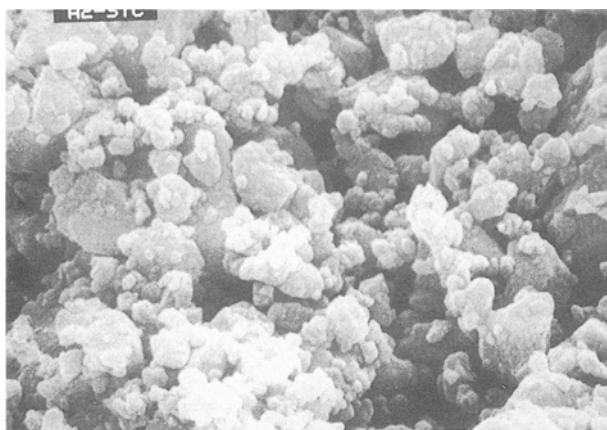


Figure 1 0.7 μm "spherical" filler.

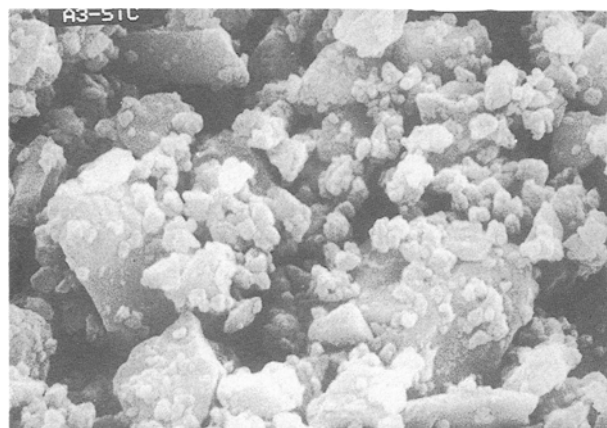


Figure 2 1.5 μm "spherical" filler.

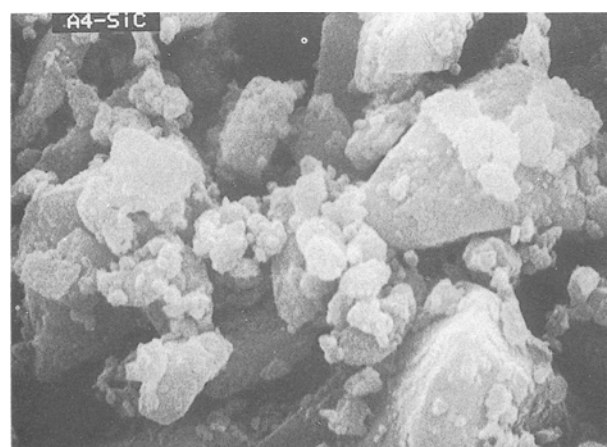


Figure 3 6 μm "spherical" filler.

Particulate composites, that is, composites containing particulate silicon carbide only, were also fabricated under the same conditions as the hybrid composites. These composites were tested to determine the matrix properties for the hybrids. Each composite specimen was tested in four-point flexure at room temperature with 20 mm, 64 mm spans to obtain microcrack stress and strain and ultimate strength. The transverse strength was also measured in flexure under the same conditions. The composite



Figure 4 Abrasive 5 μm powder.

specimens were surface ground to 2 mm thickness and cut to 3 mm width. The interlaminar shear strength was measured by short-beam shear test in three-point bending with a 6.4 mm span. The fracture toughness of the particulate composites was measured by single-edge notched beam (SENB) technique. This technique was chosen because of its simplicity, and because it had been shown earlier that the SENB technique gives the same fracture toughness values as the chevron notch technique for filled glass systems [11].

## 4. Results and discussion

### 4.1. Particulate-reinforced matrix

Initial experiments were done with particulate composites. Fracture toughness and modulus of rupture (MOR) measurements were carried out on composites with 5, 7.5 and 10 wt % particulate fillers of the 0.7, 1.5 and 6 μm mean particle size. The properties of these composites are given in Table I. As seen from the data, the fracture toughness increases from 1.0 MPa m<sup>1/2</sup> for the unreinforced matrix, to 1.485 MPa m<sup>1/2</sup> at 5 wt % filler loading for the 6 μm filler size. At higher filler loadings the fracture toughness does not increase substantially. At 7.5 and 10 wt % loading, fracture toughness is 1.606 and 1.665 MPa m<sup>1/2</sup>, respectively. Fig. 5 shows the variation of the fracture toughness with filler loading.

For the 1.5 and 0.7 μm filler loaded composites, the fracture toughness data shows the same trends. The fracture toughness increases substantially at 5 wt % filler loading, but does not increase significantly as the

TABLE I Mechanical properties of particulate composites

Mean particle size (μm)	Particle content (wt %)	Fracture toughness (MPa m <sup>1/2</sup> )	MOR (MPa)
6	0.0	1.1 (± 0.022)	49.60 (± 7.5)
	5.0	1.485 (± 0.033)	74.40 (± 4.13)
	7.5	1.606 (± 0.09)	82.68 (± 1.37)
	10	1.665 (± 0.08)	77.85 (± 0.68)
1.5	5.0	1.58 (± 0.033)	74.40 (± 2.06)
	7.5	1.595 (± 0.11)	76.47 (± 2.75)
	10	1.727 (± 0.088)	83.36 (± 4.13)
0.7	5.0	1.408 (± 0.066)	64.07 (± 6.89)
	7.5	1.408 (± 0.26)	78.54 (± 7.5)

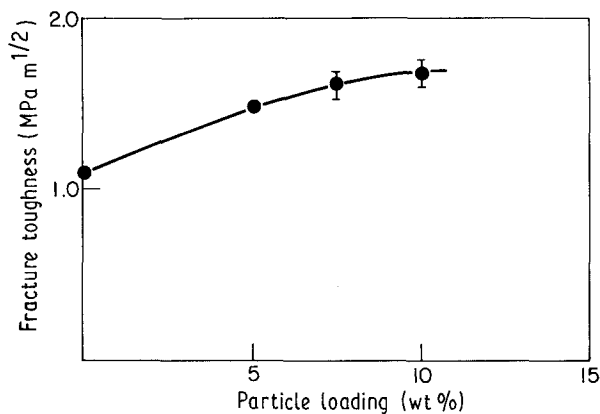


Figure 5 Fracture toughness of particulate composites (6  $\mu\text{m}$  particles).

loading is increased to 7.5 and 10 wt%. The fracture toughness improvement obtained with 0.7  $\mu\text{m}$  fillers is less than the improvement obtained with 1.5 or 6  $\mu\text{m}$  filler sizes. At 5 wt% filler loading, for example, the fracture toughness obtained with 0.7  $\mu\text{m}$  filler is 1.408  $\text{MPa m}^{1/2}$  compared with 1.58 and 1.485  $\text{MPa m}^{1/2}$  obtained for 1.5 and 6  $\mu\text{m}$  filler sizes, respectively. Interestingly the fracture toughness obtained for 1.5  $\mu\text{m}$  filler composite is higher than for the 6  $\mu\text{m}$  filler composite.

Calculations can be carried out with these known data to predict expected increases in microcrack stress from Equation 1. Table II shows these data. It is concluded that 40%–70% increases in microcrack stress can be obtained by particulate reinforcement of the matrix. These improvements, although not as high as that obtained with silicon carbide whiskers, are still very significant. Particulate loadings higher than 10 wt% were not evaluated because the composite consolidation becomes very difficult for hybrid composites with such high filler loadings.

The modulus of rupture or flexural strength data for the particulate composites are also given in Table I. There is a substantial increase in the strength of the composites compared to the strength of the unreinforced matrix composites. For 6  $\mu\text{m}$  filler size the composite strength increases from 49.6 MPa to 74.4 MPa at 5 wt% filler loading, an increase of about 50%. In similar behaviour to that of the fracture toughness, the strength does not go up substantially on increasing the particulate loading to 7.5 and 10 wt%. The MOR of the particulate composites does not appear to be a

TABLE II Predicted microcrack stress for particulate hybrids

Mean particle size ( $\mu\text{m}$ )	Particle loading (wt %)	Predicted microcrack stress (MPa)	$\left( \frac{\sigma_{\text{mcy-hybrid}}}{\sigma_{\text{mcy-nonhybrid}}} \right)$
6	5.0	459.96	1.483
	7.5	497.44	1.604
	10	511.07	1.648
1.5	5.0	490.6	1.582
	7.5	494.0	1.593
	10	534.9	1.725
0.7	5.0	436.11	1.406
	7.5	436.11	1.406

strong function of particle size. At 5 wt% loading the MOR of 6, 1.5 and 0.7  $\mu\text{m}$  size particle filled composites is 74.4, 74.4 and 64.07 MPa, respectively, and at 7.5 wt% loading it is 82.68, 76.47 and 78.54 MPa, respectively. As seen from Equation 2, the transverse strength of the hybrids is expected to be directly proportional to the particulate-reinforced matrix strength. Thus it is expected that the transverse strength would not be significantly affected by the particle size or the volume fraction of particles in the size range studied. Interlaminar shear strength also should follow the same pattern.

## 4.2. Hybrid composites

Hybrid composites were fabricated with the particulate mixed matrices as described before and their mechanical properties, i.e. microcrack stress and strain, ultimate strength and strain, and interlaminar shear strength as well as transverse strength were measured. The properties of the hybrids are given in Tables III–V.

### 4.2.1. Microcrack stress and ultimate strength

Table III shows the properties of hybrids with 6  $\mu\text{m}$  particulate filler. The microcrack stress increases substantially from 310 MPa for non-hybrid to 482 MPa at 5 wt% filler loading. The microcrack stress increases slightly to 503 MPa as loading is increased further to 7.5 wt%, and then decreases to 434 MPa at 10 wt% loading. As shown in Table II, the microcrack stress is expected to increase by 48% at 5 wt% loading. As the loading increases the microcrack stress is expected to increase by 60% at 7.5 wt% loading and by 65% at 10 wt% filler loading. The data, however, show that microcrack stress is maximum at 7.5 wt% loading and begins to decline at higher loading levels. The observed trends in the data are the same as those observed for whisker–fibre hybrids [6]. In the whisker–fibre hybrid case also, an optimum in microcrack stress was observed at 10 wt% whisker loading, although theory predicted a continuous increase in microcrack stress with increasing whisker loading level. The explanation in the whisker–fibre hybrid case for the deviation of the actual behaviour from theory was that substantial damage was inflicted on the fibres by the whiskers, and, at high whisker loading levels, the composite essentially acted as a short fibre composite. The possible explanation for this particulate–fibre hybrid system is discussed later in the paper.

The ultimate strength of the composites declines on hybridization from 827 MPa to 689 MPa at 5 wt% loading level and increases again to 778 MPa at 7.5 wt% loading and then declines to 537 MPa at 10 wt% loading. The increase in strength at 7.5 wt% loading compared to 5 wt% loading may be attributed to strength variations within a given fibre lot, and not to a fundamentally new phenomenon. The ultimate strengths of the hybrid composites are, in general, lower for hybrids compared to those of non-hybrid composites. The ultimate failure strain also

TABLE III Mechanical properties of hybrid containing 6  $\mu\text{m}$  filler

Filler (wt %)	$\sigma_{mcy}$ (MPa)	$\epsilon_{mcy}$ (%)	$\sigma_{ult}$ (MPa)	$\epsilon_{ult}$ (%)	$\sigma_T$ (MPa)	ILSS <sup>a</sup> (MPa)
0	310 ( $\pm 15$ )	0.23 ( $\pm 0.011$ )	827 ( $\pm 50$ )	1.1 ( $\pm 0.10$ )	10.4 ( $\pm 2$ )	48.2 ( $\pm 5$ )
5	482 ( $\pm 20$ )	0.30 ( $\pm 0.012$ )	689 ( $\pm 62$ )	0.63 ( $\pm 0.08$ )	55 ( $\pm 6$ )	103 ( $\pm 8$ )
7.5	503 ( $\pm 17$ )	0.31 ( $\pm 0.010$ )	778 ( $\pm 61$ )	0.64 ( $\pm 0.05$ )	75.8 ( $\pm 9$ )	145 ( $\pm 11$ )
10	434 ( $\pm 16$ )	0.28 ( $\pm 0.010$ )	537 ( $\pm 48$ )	0.56 ( $\pm 0.072$ )	48 ( $\pm 6$ )	124 ( $\pm 15$ )
5 (5 $\mu\text{m}$ abrasive grain)	427 ( $\pm 21$ )	0.34 ( $\pm 0.016$ )	503 ( $\pm 24$ )	0.43 ( $\pm 0.02$ )	31.7 ( $\pm 3$ )	101 ( $\pm 9$ )

<sup>a</sup> Interlaminar shear strength.

TABLE IV Mechanical properties of hybrids containing 1.5  $\mu\text{m}$  filler

Filler (wt %)	$\sigma_{mcy}$ (MPa)	$\epsilon_{mcy}$ (%)	$\sigma_{ult}$ (MPa)	$\epsilon_{ult}$ (%)	$\sigma_T$ (MPa)	ILSS <sup>a</sup> (MPa)
0	310 ( $\pm 15$ )	0.23 ( $\pm 0.011$ )	827 ( $\pm 50$ )	1.1 ( $\pm 0.10$ )	10.4 ( $\pm 2$ )	48.2 ( $\pm 5$ )
5	344.5 ( $\pm 26$ )	0.26 ( $\pm 0.02$ )	633.9 ( $\pm 35$ )	0.53 ( $\pm 0.015$ )	71.6 ( $\pm 10$ )	100.0 ( $\pm 8$ )
7.5	379.0 ( $\pm 32$ )	0.29 ( $\pm 0.025$ )	654.5 ( $\pm 50$ )	0.53 ( $\pm 0.02$ )	62 ( $\pm 8.5$ )	134.3 ( $\pm 11$ )
10	275.0 ( $\pm 24$ )	0.23 ( $\pm 0.021$ )	516.7 ( $\pm 43$ )	0.50 ( $\pm 0.008$ )	55 ( $\pm 9$ )	126.8 ( $\pm 12$ )

<sup>a</sup> Interlaminar shear strength.

TABLE V Mechanical properties of hybrids containing 0.7  $\mu\text{m}$  filler

Filler (wt %)	$\sigma_{mcy}$ (MPa)	$\epsilon_{mcy}$ (%)	$\sigma_{ult}$ (MPa)	$\epsilon_{ult}$ (%)	$\sigma_T$ (MPa)	ILSS <sup>a</sup> (MPa)
0	310 ( $\pm 15$ )	0.23 ( $\pm 0.011$ )	827 ( $\pm 50$ )	1.1 ( $\pm 0.10$ )	10.4 ( $\pm 2$ )	48.2 ( $\pm 5$ )
5	330.7 ( $\pm 26$ )	0.25 ( $\pm 0.02$ )	400 ( $\pm 42$ )	0.34 ( $\pm 0.028$ )	64.7 ( $\pm 9$ )	80.0 ( $\pm 15$ )
7.5	273.6 ( $\pm 23$ )	0.21 ( $\pm 0.018$ )	289.3 ( $\pm 25$ )	0.21 ( $\pm 0.02$ )	55.1 ( $\pm 7.5$ )	46.8 ( $\pm 6$ )

<sup>a</sup> Interlaminar shear strength.

declines from 1.1% to 0.63% at 5 wt% filler loading, remains at 0.64% at 7.5 wt% loading and declines to 0.56% at 10 wt% loading. There is probably some damage to fibres within the particulate hybrids as in the case of whisker hybrids. Fig. 6 shows the microcrack and ultimate strength data for the 6  $\mu\text{m}$  filler as a function of particle loading.

Table III also provides data for hybrids containing 5  $\mu\text{m}$  abrasive grain silicon carbide powder with sharp edged particles. It is clear that the microcrack stress, ultimate strength and ultimate strain are all substantially lower for the abrasive grain composite compared to the composite with 5 wt% 6  $\mu\text{m}$  spherical filler loading. These data indicate that the rounded edges on the spherical fillers are indeed beneficial in reducing fibre damage and matrix stress concentrations. Although the data cannot be directly compared because of the difference in particle size, the sizes are close enough for the above conclusion to be reasonable.

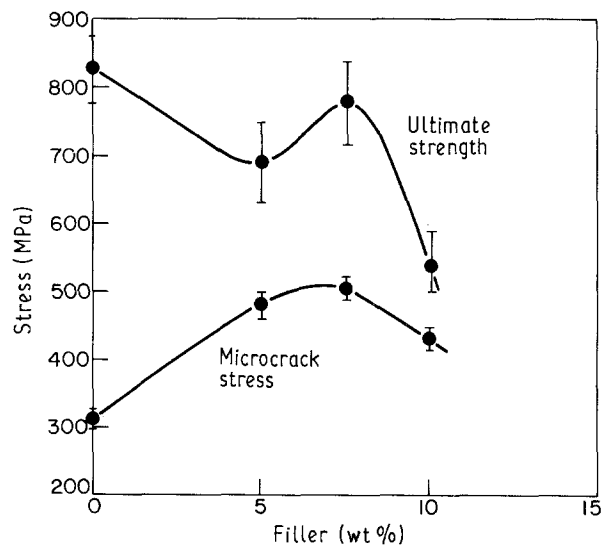


Figure 6 Variation of microcrack stress and ultimate strength as a function of filler loading level (6  $\mu\text{m}$  particles).

The data for hybrids containing 1.5  $\mu\text{m}$  filler are given in Table IV. The microcrack stress increases from 310 MPa for no filler loading to 344 MPa for 5 wt% filler loading and to 379 MPa for 7.5 wt% filler loading. At 10 wt% filler loading, however, the microcrack stress declines to 275 MPa, even lower than that for the unfilled matrix. The data thus show trends similar to that of the data for 6  $\mu\text{m}$  filler size with an optimum loading level at 7.5 wt% filler. The improvements obtained in microcrack stress, however, are substantially lower than in the case of 6  $\mu\text{m}$  filler. The ultimate failure strengths and ultimate strains are also higher for 6  $\mu\text{m}$  filler hybrids than 1.5  $\mu\text{m}$  filler hybrids. The predictions in Table II indicate that the microcrack stress improvement obtained with 1.5  $\mu\text{m}$  filler size should be equal to or higher than the improvement obtained with 6  $\mu\text{m}$  filler at equivalent loading level. The results are, however, contrary to the predictions.

Table V shows the data for 0.7  $\mu\text{m}$  filler containing hybrids. The microcrack stress has increased slightly to 330 MPa at 5 wt% loading level, and declines to 273 MPa at 7.5 wt% loading compared to 310 MPa for a non-hybrid composite. Ultimate failure strength declines from 827 MPa to 400 MPa at 5 wt% loading and further to 289 MPa at 7.5 wt% loading. The ultimate failure strain also decreases from 1.1% to 0.34% at 5 wt% loading level. At this particle size, there is a minimal increase in microcrack stress accompanied by a large drop in ultimate strength and strain properties.

Fig. 7 shows the variation of microcrack stress as a function of particle size at 7.5 wt% filler loading. The microcrack stress is highest for 6  $\mu\text{m}$  filler size. It increases by 62% from 310 MPa for a non-hybrid to 503 MPa for the hybrid. The trend in the data for microcrack stress as a function of particle size is very different from that predicted in Table II. These differences can be summarized as follows,

1. An optimum in microcrack stress is obtained.
2. The ultimate strength and strains of the hybrids are lower than those of non-hybrids.
3. Particle size appears to have a significant effect on microcrack stress, with the largest particles resulting in highest microcrack stress and also highest ultimate strengths and strains for the hybrid composites.

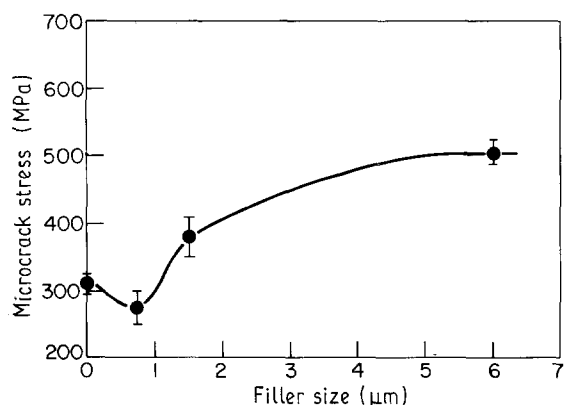


Figure 7 Variation of microcrack stress as a function of filler size.

The first and second observations indicate trends similar to those for whisker-fibre hybrids [6]. Such trends in the case of whisker-fibre hybrids are related to the fibre damage induced by the whiskers, the frequency of which increased with increased whisker loading. Major fibre damage was not expected for the particulate loading. The fracture surfaces were examined to verify this assumption.

Fig. 8 shows scanning electron micrographs of fracture surfaces of non-hybrid, and 7.5 wt% loaded hybrid composites with 0.7 and 6  $\mu\text{m}$  particles, respectively. The micrographs indicate clearly that the very fibrous fracture surface of the non-hybrid composite changes to a woody fracture at 6  $\mu\text{m}$  particle loading. With the 0.7  $\mu\text{m}$  particle loading, the fracture surface becomes brittle with almost no visible pull-out of fibres. A close examination of the fracture surfaces of particulate hybrids was carried out using SEM, and are shown in Fig. 9. The fibres clearly show damaged graphitic skin, which is the main cause of

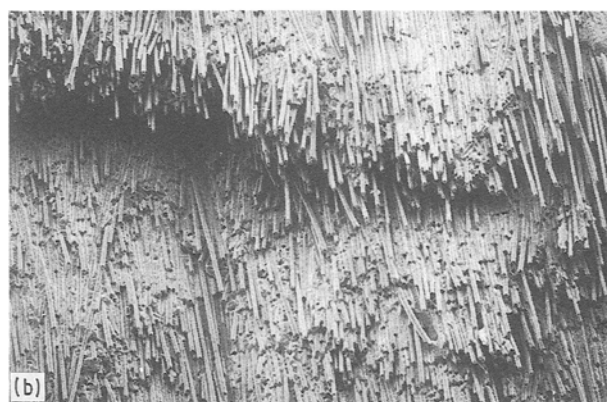
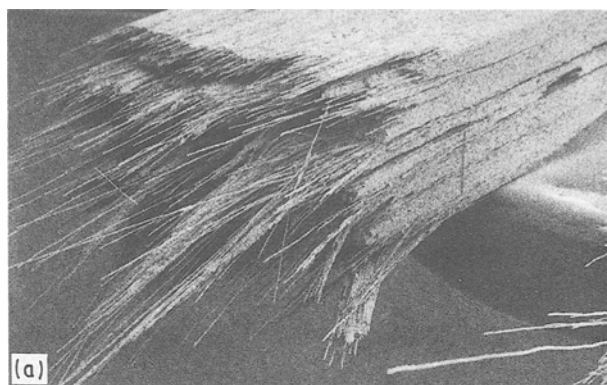


Figure 8 Comparison of fracture surfaces of hybrid composites.

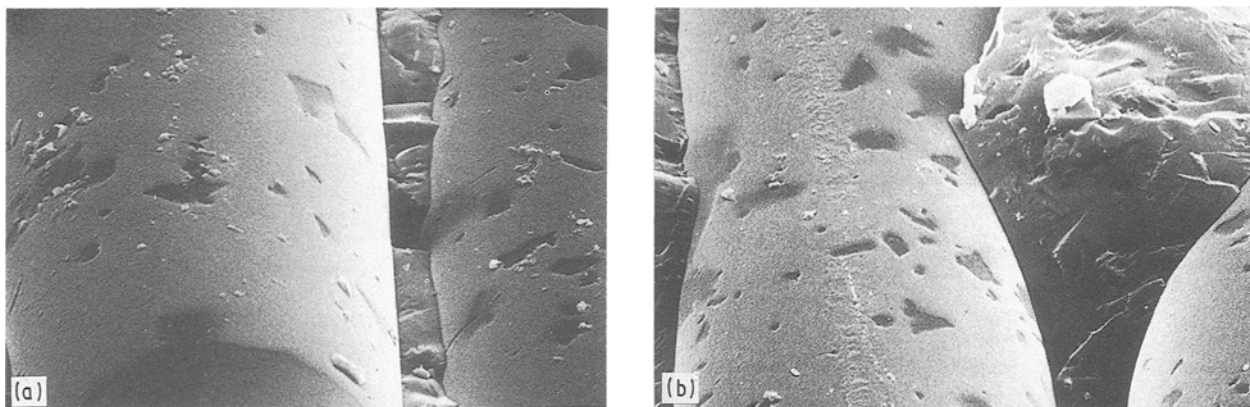


Figure 9 Fracture surfaces of the hybrids showing damaged graphitic interfaces.

weak bonding between the fibre and the matrix. The graphitic skin results in high failure strain, high-strength composites with long fibre pull-out on the fracture surface. The particulate fillers are in contact with the fibres during processing and, either prevent formation of the graphitic skin at contact points, or damage the already formed skin during processing. Damage to the graphitic skin would then result in lower ultimate strengths and strains. It is interesting to note that the fillers damage the graphitic interface but do not physically damage the fibres as in the case of whisker hybrids.

The third observation that the microcrack stress as well as ultimate strength and strain are higher for larger particle sizes can be rationalized as follows. As seen from the micrographs, the presence of particulates results in the absence of a graphitic interface at the contact points between the particulate and the fibre. This, in turn, results in lower ultimate properties of the composite with small pull-out lengths and brittle failure. It is anticipated that with an increase in the number of contact points, the properties will decline more. At a given volume per cent, the number of particles of a given material is inversely proportional to the square of the ratio of their diameters. It is then easily calculated that for every 6  $\mu\text{m}$  particle there are about 16 particles of 1.5  $\mu\text{m}$  diameter and 60 particles of 0.77  $\mu\text{m}$  diameter. The frequency of contact points may be expected to be directly proportional to the number of particles. As the particle size decreases, the number of contact points increases substantially, resulting in a higher proportion of damage to the graphitic skin, which, in turn, results in lower mechanical properties. This argument supports the conclusion that larger filler particle sizes produce better hybrid composite properties. In practice, however, an upper limit on the particle size rests on process considerations and the need to have an optimum interparticle distance. The latter causes pinning and bending of the crack front which results in a higher fracture toughness of the matrix. If the particle size exceeds a certain maximum, at the allowable volume fraction of particles in the matrix, there may be little or no improvement in fracture toughness. This would result in no improvement in microcrack stress, as explained earlier, thereby negating the purpose of hybridization.

#### 4.2.2. Transverse strength and interlaminar shear strength

The effect of the 6  $\mu\text{m}$  particle size filler loading on the transverse strength and interlaminar shear strength of the hybrid is shown in Fig. 10. The transverse strength increases five-fold from 10 MPa to 55 MPa at 5 wt% loading, and further to 75 MPa at 7.5 wt% loading. As the filler loading level increases to 10 wt%, however, the strength declines to 48 MPa. The optimum in transverse strength also is obtained at 7.5 wt% loading level, at which point the microcrack stress and ultimate strength were highest for the hybrids. Based on Equation 2 and properties of the particulate matrices given in Table I, improvements of 50–60% in transverse strengths were expected for hybrid composites compared to non-hybrids. Observed improvements are substantially higher. The transverse strength obtained at 7.5 wt% loading is about the same as for the particulate matrix strength. In expecting improvements of 50–60% in transverse strength it was assumed that the stress concentration factor derived from the presence of weakly bonded fibres would not be affected because of the particulate loading. It appears that the effect of these stress concentration factors are substantially reduced. Any

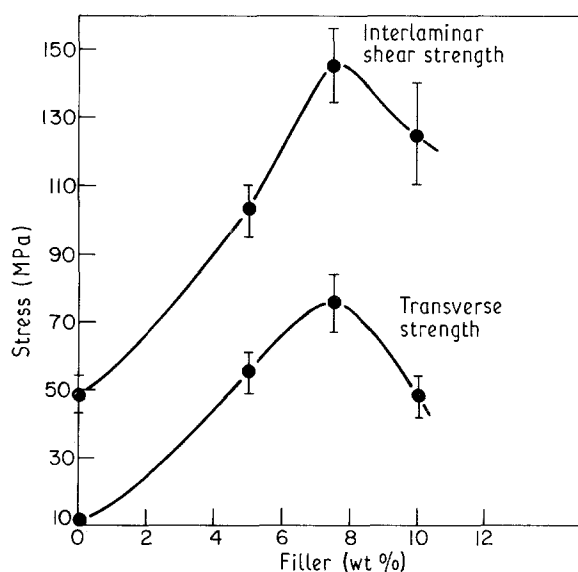


Figure 10 Transverse and interlaminar shear strength of hybrids as a function of filler loading (6  $\mu\text{m}$  filler).

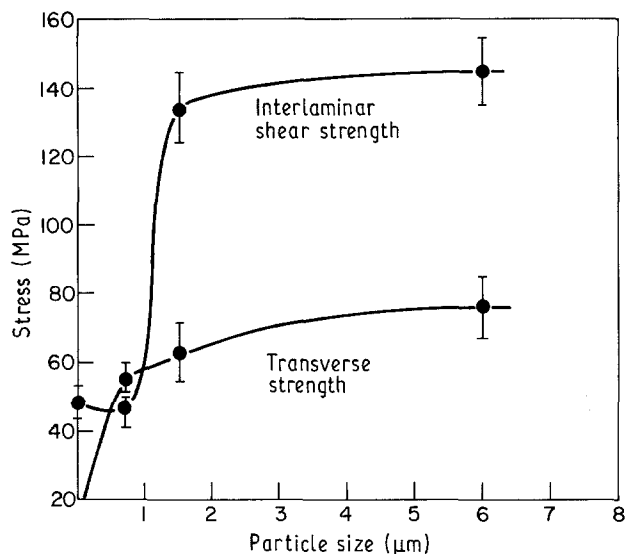


Figure 11 Transverse and interlaminar shear strength as a function of filler size.

strength-limiting flaws that initiate at these weak interfaces are effectively stopped by the fillers which results in transverse strengths equivalent to matrix strengths. The resistance to flaw propagation appears to be optimum at 7.5 wt% loading for the hybrids.

The interlaminar shear and transverse strengths show the same trends. The interlaminar shear strength doubles at 5 wt% loading from 48 MPa to 103 MPa, and attains a maximum value of 145 MPa at 7.5 wt% loading. Since interlaminar shear strength is also affected by the same parameters, i.e. the matrix strength and the bond strength between the fibre and the matrix, a maximum in interlaminar shear strength is expected at the maximum for transverse strength. The data clearly show the maximum in both strengths occurs around the 7.5 wt% loading level.

It is suggested that the decline in the composite properties beyond 7.5 wt% loading is related to the consolidation problems associated with the highly loaded composites. At high loading levels there would be agglomeration of particles and poor matrix infiltration. Such agglomerates would be the failure initiation sites which result in lower strengths. This problem should become more severe at high loadings of smaller particle size filler.

Fig. 10 shows the transverse and interlaminar shear strengths as a function of filler size at 7.5 wt% loading level. The transverse strength increases from 10 MPa to 55 MPa at 0.77 μm filler size, to 62 MPa at 1.5 μm filler size, and to 76 MPa at 6 μm filler size. The particulate matrix strengths given in Table II at this loading level are about the same irrespective of the particle size. As indicated before, the data point to a possible agglomeration problem with smaller particle sizes. With both 1.5 and 0.77 μm particles, the transverse strength of the hybrids declines with increasing loading level. For the 1.5 μm filler, the strength declines from 72 MPa at 5 wt% loading, to 62 MPa at 7.5 wt% loading, and to 55 MPa at 10 wt% loading.

The interlaminar shear strength also shows similar trends as a function of particle size. The interlaminar shear strength at 7.5 wt% loading is shown in Fig. 10 as a function of particle size. The strength increases from 48 MPa to 145 MPa for the 6 μm particle size. Table V shows that the interlaminar shear strength increases from 48 MPa for non-hybrid to 80 MPa at 5 wt% loading of 0.77 μm particles. As the loading increases to 7.5 wt%, however, the strength declines to 47 MPa. The higher loading level with the smaller particle sizes is thus detrimental to composite properties.

## 5. Conclusions

Hybridization of the fibre-reinforced glass matrix composites with particulate fillers results in substantial improvements in microcrack stress, transverse strength and interlaminar shear strength. The ultimate strengths and strains decline on hybridization. It was found that the presence of particles results in either prevention of formation of the graphitic skin or damage to the already formed skin, with a resultant decrease in ultimate properties.

The microcrack stress, off-axis properties, and ultimate properties improve with increase in particle size at a given volume fraction. Lower contact frequency between the fibre and the particulate with the smaller number of the larger particles is thought to be the reason for this trend in behaviour. Truly spherical particles with a narrow size distribution and a 6–10 μm mean particle size might result in significant improvements over that reported here.

## Acknowledgements

The author thanks J. Mach and the Composites Fabrication Center staff for their help in composite fabrication, and K. P. Reddy, W. Vann and J. Bartoo for their help in testing and analysis of the data.

## References

1. J. J. BRENNAN and K. M. PREWO, *J. Mater. Sci.* **17** (1982) 2371.
2. K. M. PREWO, *ibid.* **22** (1987) 2695.
3. K. M. PREWO and J. J. BRENNAN, *ibid.* **15** (1980) 463.
4. R. F. COOPER and K. CHYUNG, *ibid.* **22** (1987) 3148.
5. D. M. DAWSON, R. F. PRESTON and A. PURSER, *Silicate Industrials* **53** (1988) 129.
6. K. P. GADKAREE, K. C. CHYUNG and M. P. TAYLOR, *J. Mater. Sci.* **23** (1988) 3711.
7. J. FRIEDEL, in "Fracture", edited by B. L. Averbach *et al.* (Wiley, New York, 1959) p. 498.
8. F. F. LANGE, *Phil. Mag.* **22** (1970) 983.
9. F. F. LANGE and K. C. REDFORD, *J. Mater. Sci.* **6** (1971) 1197.
10. L. J. BRAUTMAN and S. SAHU, in "Proceedings of the 26th Annual Technical Conference on Reinforced Plastics" (SPI, 1971) p. 14C.
11. K. P. R. REDDY and K. P. GADKAREE, in "Proceedings of the XIV International Glass Congress" (Indian Ceramic Society, Calcutta, 1986) p. 270.

Received 21 March  
and accepted 1 July 1991